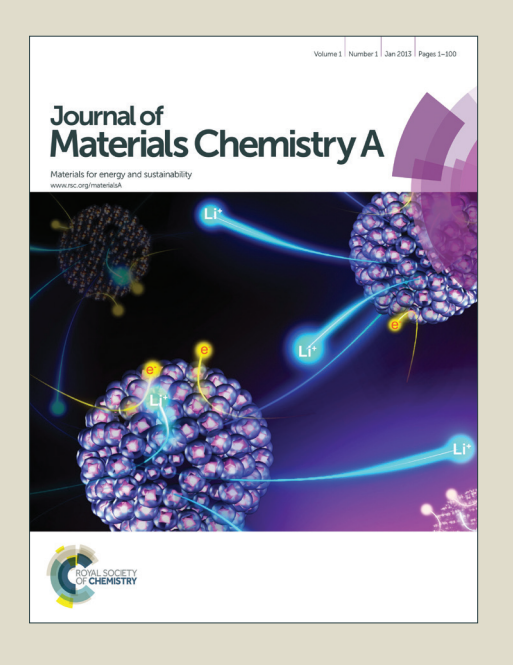
Journal of Materials Chemistry A

Accepted Manuscript



This is an *Accepted Manuscript*, which has been through the Royal Society of Chemistry peer review process and has been accepted for publication.

Accepted Manuscripts are published online shortly after acceptance, before technical editing, formatting and proof reading. Using this free service, authors can make their results available to the community, in citable form, before we publish the edited article. We will replace this Accepted Manuscript with the edited and formatted Advance Article as soon as it is available.

You can find more information about *Accepted Manuscripts* in the **Information for Authors**.

Please note that technical editing may introduce minor changes to the text and/or graphics, which may alter content. The journal's standard <u>Terms & Conditions</u> and the <u>Ethical guidelines</u> still apply. In no event shall the Royal Society of Chemistry be held responsible for any errors or omissions in this *Accepted Manuscript* or any consequences arising from the use of any information it contains

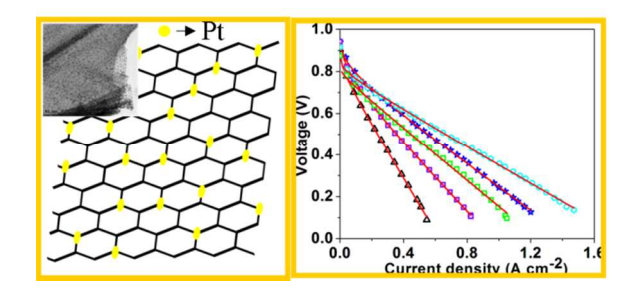


Platinum-Graphene hybrid nanostructure as anode and cathode electrocatalyst in proton exchange membrane fuel cell

Divya P. and Ramaprabhu S.

Alternative Energy and Nanotechnology Laboratory (AENL), Nano Functional Materials Technology centre (NFMTC), Department of Physics, Indian Institute of Technology Madras, India. * Phone: +91-44-22574862; E-mail: ramp@iitm.ac.in

Graphical abstract with text



Graphene synthesized by an environmentally benign technique is applied as a low cost electrocatalyst support in proton exchange membrane fuel cell.

Cite this: DOI: 10.1039/c0xx00000x

www.rsc.org/xxxxxx

ARTICLE TYPE

Platinum - Graphene hybrid nanostructure as anode and cathode electrocatalyst in proton exchange membrane fuel cell

Divya P. and Ramaprabhu S.

Received (in XXX, XXX) XthXXXXXXXXX 20XX, Accepted Xth XXXXXXXX 20XX 5 DOI: 10.1039/b000000x

ABSTRACT: In the present study, platinum nanoparticles decorated on graphene sheets have been employed as electrocatalyst for both oxygen reduction reaction and hydrogen oxidation reaction in proton exchange membrane fuel cell. A green and simple approach has been followed for the reduction of graphite oxide using L-ascorbic acid (L-ARGO). Platinum nanoparticle decoration on graphene (Pt/L-ARGO) sheets has been carried out by polyol reduction technique. The structural and morphological characterizations have been done by different characterization techniques to confirm the formation of materials. The power densities have been evaluated from the recorded polarization curves. The single cell measurements show that the electrocatalytic activity of Pt/L-ARGO is superior in comparison to chemically reduced Pt-graphene systems.

15 1. INTRODUCTION

The rapid depletion of fossil fuels and noxious emissions due to their consumption has triggered significant interest in development of alternate energy based conversion devices. Proton exchange membrane fuel cells (PEMFCs) are one of the 20 promising energy conversion devices that can extract electrical energy from chemical reactions with only water as the byproduct¹. High catalytic activity of the noble metal platinum at anode and cathode ensures oxidation and reduction of fuel and oxidant respectively to generate electricity and water in PEMFC. 25 Major shortcomings hindering the successful commercialization of PEMFC are sluggish oxygen reduction reaction (ORR) kinetics, low abundance and cost of platinum². Hence, efficient usage of platinum (Pt) electrocatalyst is essential to commercialize fuel cells rapidly³. The electrocatalytic activity of 30 platinum can be improved by engineering its morphology, alloying or making composites⁴.

Recent research has focused mainly on the enhancement in the performance of fuel cell by minimizing the platinum content by depositing it on catalyst support materials. An ideal ³⁵ electrocatalyst support must have high electrical conductivity for fast electron transport to the collecting electrodes, good chemical stability under normal PEMFC conditions to ensure long term operation, strong affinity towards the catalyst particles and high surface area and porosity. The moderate electrical conductivity ⁴⁰ and surface area of carbon black (Vulcan XC 72) has made it a state-of-the-art electrocatalyst support in proton exchange membrane fuel cell. However, electrochemical oxidation and weak binding of platinum nanoparticles with carbon black results in the detachment of platinum particles causing aggregation. This ⁴⁵ leads to degradation in the performance as well as low durability of fuel cells^{5, 6}. Considerable efforts have been devoted to the

development of alternative electrocatalyst supports. Discovery of the one dimensional allotrope of carbon, carbon nanotubes by Ijima in 1991⁷ opened a new era in science and engineering. 50 Unique electrical and electronic properties, wide electrochemical window and high surface area prompted researchers to employ carbon nanotubes in energy conversion devices such as solar cells 8, supercapacitors⁹, lithium ion batteries¹⁰. Application of carbon nanotubes as an electrocatalyst support in fuel cell is extensively 55 reported in literature 11-14. Hydrophobic surface of carbon nanotubes are not favourable for most of the applications. Acid treatment is a known technique, which is employed to get anchoring sites such as carboxylic, and hydroxyl functional groups for metal decoration on carbon nanotubes^{15, 16}. 60 Experimental realization of graphene in 2004¹⁷ by micro mechanical cleavage has made it a revolutionary material in numerous disciplines. Most of the applications demand largescale synthesis of graphene. A clean solution to solve this issue is exfoliation of chemically modified form of graphite, graphite 65 oxide. Several techniques such as hydrogen exfoliation 18, focused solar exfoliation¹⁹, thermal exfoliation, vacuum exfoliation²⁰ and chemical reduction^{21, 22} have been reported. The discovery of the graphene sheets has opened the possibility of a new low cost electrocatalyst support for holding platinum nanoparticles. 70 Graphene sheets prepared by some of the exfoliation techniques have already been explored as electrocatalyst support in fuel cells²³⁻²⁸. There is a significant challenge hidden in the selection of method adopted to get uniform anchoring of Pt nanopatricles on electrocatalyst supports, which will greatly influence the fuel 75 cell performance. Polyol reduction method has been found to be exceptionally good for anchoring Pt nanoparticles on functionalized carbon nanotubes as well as graphene^{14, 28}.

In the present work, an easy and green-technique was chosen for mass production of graphene from graphite oxide. This graphene was employed as an electrocatalyst support in anode as well as cathode of PEMFC. Multiwalled carbon nanotubes (MWNT) synthesized by catalytic chemical vapour deposition (CCVD) technique is the alternative electrocatalyst support 5 employed in the present study. Pt nanoparticles were dispersed on graphene and functionalized MWNT by polyol reduction method. Single cell measurements of a series of membrane electrode assemblies were carried out to briefly examine the ORR activity of the prepared materials. The present work also briefly explains 10 the hydrogen oxidation reaction (HOR) activity of platinum decorated graphene through single cell measurement and the result is compared with the same activity of Pt decorated MWNT (Pt/f-MWNT).

2. EXPERIMENTAL SECTION

15 2.1 Materials

Graphite used was purchased from sigma Aldrich. Sodium Nitrate (NaNO₃, 99.5%), Potassium Permanganate (KMnO₄, 99.5%) and concentrated sulphuric acid (H₂SO₄, 98%) were purchased from Rankem chemicals, India. Hydrogen Peroxide ²⁰ (30%) was procured from SD Fine-Chem ltd India. Hexachloroplatinic acid (H₂PtCl₆.6H₂O) was purchased from Sigma-Aldrich and ethylene glycol was purchased from Merck. DI water was used for all reactions.

2.2 Materials synthesis

Graphite oxide (GO) was prepared by Hummers' method²⁹. The detailed experimental procedure followed is as follows. 2 g of graphite was added slowly to 46 ml of conc. H₂SO₄ under continuous stirring in an ice bath. There after 1 g NaNO3 and 6 g KMnO₄ were added one after another. The suspension was taken 30 out from the ice bath and allowed to cool down to room temperature. Then 92 ml of water was added to above mixture. After 15 min, 280 ml warm water was added to dilute the mixture. Further 3% H₂O₂ was added to get yellow coloured suspension. The suspension was filtered and washed with warm 35 water, repeatedly. The product was diluted using water and the resulting suspension was centrifuged. The final product was dried under vacuum and stored in vacuum desiccators, for further use. Graphene sheets were synthesized by reducing GO by L-ascorbic acid³⁰. 100 mg of GO was dispersed in water and aqueous 40 solution of L-ascorbic acid was added to the above solution drop by drop under vigorous stirring. Further the solution was stirred vigorously for 20 h. The temperature maintained was 30 °C. The resultant sample was washed with copious amount of DI water, filtered and dried in vacuum oven, kept in vacuum desiccator for 45 further use, named as L-ARGO. Required amount of L-ARGO was dispersed in ethylene glycol by ultrasonication and 1 wt% hexachloroplatinic acid was added under stirring to get loading of platinum on L-ARGO. Platinum nanoparticles formed by refluxing the above solution at 130 °C for 4h.

50 MWNT were synthesized by catalytic chemical vapour deposition of carbon precursor, acetylene over AB₃ (A= misch metal, B=Ni) based alloy hydride catalyst ³¹. As grown MWNT were purified by air oxidation at 400 °C, which remove the amorphous carbon deposited during the growth process. The 55 catalytic impurities were removed by refluxing the sample in concentrated nitric acid for 24 h. Further, the sample was washed

and dried in vacuum oven at 60 °C. MWNT were functionalized by ultrasonicating the sample in concentrated nitric acid for 3 h followed by washing the sample to get neutral pH, dried at 60 °C, named as f-MWNT and kept in a desiccator until further use. Required amount of f-MWNT was dispersed in ethylene glycol by ultrasonication. 1 wt% hexachloroplatinic acid was added to f-MWNT dispersion kept under stirring, to get loading of platinum on f-MWNT. The precursor was reduced to platinum nanoparticles by refluxing the above solution at 130 °C for 4 h. The sample was washed with DI water several times to remove ethylene glycol, dried at 60 °C, kept in desiccator for further use.

2.3 Characterizations

Powder X-ray diffraction (XRD) measurements were carried 70 out using a PANalytical X'PERT Pro X-ray Diffractometer with nickel-filtered Cu Kα radiation as the X-ray source. The pattern was recorded in the 2θ range of 5° to 90°. Identification and characterization of functional groups were carried out using PerkinElmer FT-IR spectrometer in the range 500–4000 cm⁻¹ 75 The samples were prepared by KBr pellet method. The Raman spectra were recorded using a Confocal Raman spectrometer (WITec alpha 300) with an excitation source of Nd:YAG laser (532 nm). Field emission scanning electron microscopy and transmission electron microscopy images were recorded using 80 FESEM, (FEI QUANTA 3D) operated at 30 kV and TECNAI F 20 (S-Twin) operating at 200 kV, respectively. For transmission electron microscope (TEM) image, the materials were dispersed in absolute ethanol using mild ultrasonication and cast onto carbon coated Cu grids (SPI supplies, 200 meshes). 85 Thermogravimetric analysis was carried out using a SDT Q600, TA instruments.

2.4 Preparation of electrodes and electrochemical measurement

The electrochemical experiments were carried by combining a CHI 6083 electrochemical analyzer (CH instruments) with a conventional three-electrode set up. A three electrode set up contains a Pt wire counter electrode, Ag/AgCl electrode saturated with 1M KCl as the reference electrode and a modified glassy carbon electrode as working electrode. The electrolyte used was 1M H₂SO₄. All the experiments were performed at room temperature. The working electrode is a glassy carbon electrode with a thin layer of electrocatalyst ink drop casted over it. The catalyst ink was prepared by ultrasonicating 2 mg of electrocatalyst in 100µl of ethanol for half an hour followed by adding 5µl of Nafion and ultasonicated further. Then the ink was drop casted over glassy carbon electrode using micropipette. The electrode was dried in ambient condition.

2.5 Preparation of membrane electrode assembly (MEA) and single cell measurements

The MEA is the central component of a fuel cell which is fabricated by sandwiching a Nafion 212 membrane between the anode and the cathode followed by hot pressing at 130 °C temperature and 1 ton pressure for 4 min. The Nafion membrane was pre-treated before fabrication as follows. The Nafion 212

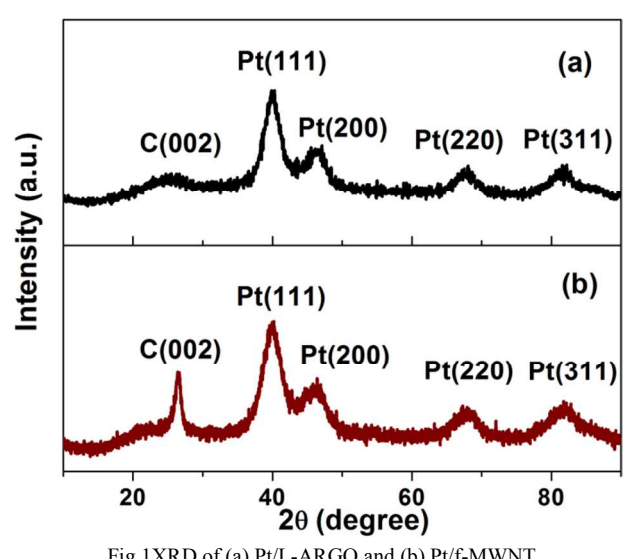


Fig. 1XRD of (a) Pt/L-ARGO and (b) Pt/f-MWNT

Table 1. Configuration of the MEAs fabricated

MEA	Anode	Anode	Cathode	Cathode
		loading		loading
		(mg cm ⁻²)		(mg cm ⁻²⁾
1	Pt/f-MWNT	0.2	Pt/L-ARGO	0.4
2	Pt/f-MWNT	0.1	Pt/L-ARGO	0.2
3	Pt/L-ARGO	0.2	Pt/L-ARGO	0.4
4	Pt/L-ARGO	0.4	Pt/f-MWNT	0.2
5	Pt/L-ARGO	0.2	Pt/f-MWNT	0.1

5 membrane was heated with 2 % H₂O₂ for 1 h at 80 °C followed by rinsing with DI water and heating with 1M H₂SO₄ for 1 h at 80 °C . There after the membrane was washed with DI water. The anode and the cathode contain a backing layer, gas diffusion layer and an electrocatalyst layer in sequence. The diffusion layer is a 10 mixture of carbon (Vulcan XC 72) and poly tetrafluoroethylene coated over a carbon cloth. Brush coating the catalyst ink made the electrocatalyst layer uniformly over the gas diffusion layer. The electrocatalyst ink was prepared by ultrasonicating, the required amount of electrocatalyst with water, isopropyl alcohol 15 and 5 wt% Nafion solution. The single cell measurement was carried out by assembling the MEA in between two graphite plates, which had a provision for gas flow (serpentine-type flow) throughout the operation. Respective mass flow controllers controlled flow rate of hydrogen and oxygen gases and the 20 incoming gases were humidified using respective humidifiers before allowing into the anode and the cathode (inline heating was provided to avoid condensation). A series of membrane electrode assemblies were fabricated and single cell measurements were carried out. Area exposed to the 25 measurement is 11.56 cm². Prior to the measurement, the electrodes were activated between OCP and 0.1 V. The details of MEAs are given in Table 1. The polarization curves were recorded at different temperatures (40, 50, and 60 °C) without backpressure and with one atmospheric pressure.

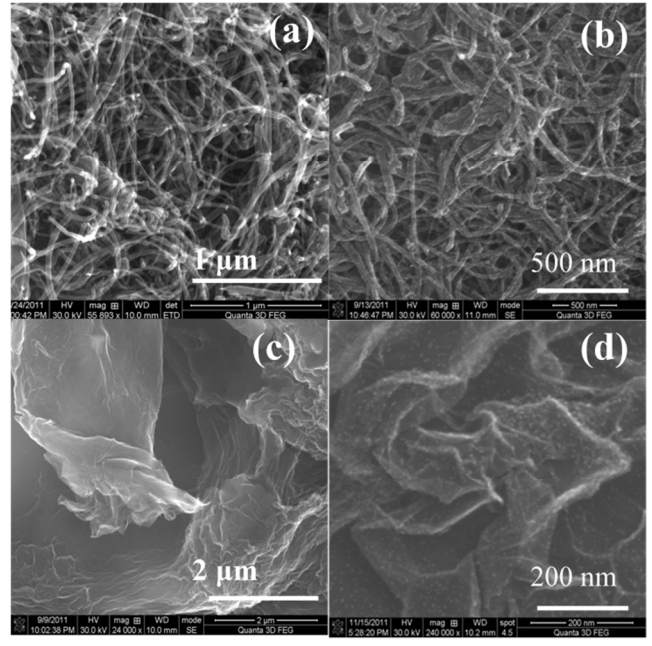


Fig.2 FESEM images of (a) MWNT,(b) Pt/f-MWNT,(c) L-ARGO and (d) Pt/L-ARGO

3. Results and discussion

Application of graphene as an electrocatalyst support needs its 35 large-scale production. This can be achieved through solution based chemical reduction of GO. Reduction of GO by environmentally friendly reducing agents needs to be explored rather than using toxic and explosive reducing agents. L- ascorbic acid is a nontoxic reducing agent. Also, L- ascorbic acid and its 40 oxidizing products are environmentally friendly³⁰. Here, Graphite oxide was synthesized by the chemical oxidation of pristine graphite and L-ascorbic acid was used to reduce GO to get L-ARGO. L-ascorbic acid releases protons and gets converted into dehydroascorbic acid. The released protons will react with 45 hydroxyl as well as epoxy groups on GO, which results in the formation of water molecules. The formed oxalic acid and gluronic acids, converted products of dehydroascorbic acid form hydrogen bonds with residual functional groups on reduced GO. This prevents the π - π stacking of the GO sheets and hence 50 agglomeration (restacking) can be avoided. 30. Pt nanoparticle decoration on L-ARGO and f-MWNT were carried out by wellknown ethylene glycol reduction, since glycolate produced by the oxidation of ethylene glycol acts as stabilizing medium for metal colloids.

55 3.1 Structural and morphological analysis

Structural features of the samples are investigated by analysing the recorded powder XRD patterns, Raman spectra and FTIRspectra of the samples. Details of XRD patterns of as grown MWNT, air oxidized MWNT, MWNT, f-MWNT, graphite, GO 60 and L-ARGO are given in †ESI (Fig. S1(a-g)). XRD of Pt/f-MWNT and Pt/L-ARGO are displayed in Fig. 1 (a&b). The strong diffraction peaks at 2θ = 39.9°, 46.1°, 67.9° and 81.9° are diffraction peaks of Pt (111), Pt (200), Pt (220) and Pt (311) planes, respectively. This confirms the formation of platinum 65 nanoparticles from Pt precursor. Also, diffraction pattern

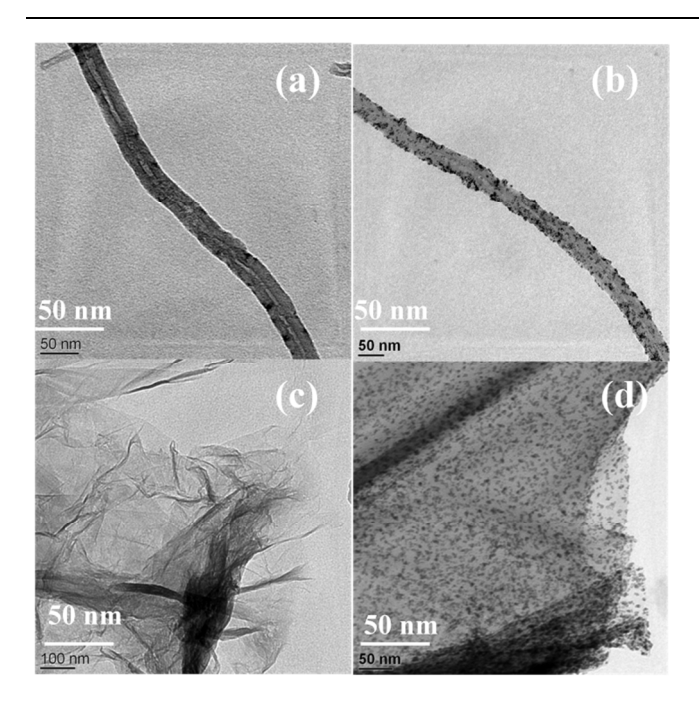


Fig.3TEM images of (a) MWNT, (b) Pt/f-MWNT, (c) L-ARGO and (d) Pt/L-ARGO

s indicates that the formed Pt nanoparticles have a face-centred cubic (fcc) structure. The peak centred at 2θ =26.5° corresponding to the hexagonal graphitic plane of the carbon support materials. MWNT are hydrophobic in nature. Attachment of functional groups by the process of acid functionalization makes the MWNT hydrophilic and provides anchoring sites for metal decoration. The FTIR and Raman spectra of MWNT, f-MWNT, graphite, GO and L-ARGO is discussed in †ESI (Fig. S2 (a-e), Fig. S3 (a-e)). Loading of platinum confirmed from TGA is 34 wt% for Pt/L-ARGO and 30 wt% for Pt/MWNT, which are shown in †ESI (Fig.S5).

The morphological and elemental analyses of the samples were carried out using scanning electron microscopy imaging, transmission electron microscopy imaging and energy dispersive X-ray analysis. FESEM images of as grown MWNT and 20 graphite are provided in supporting information for comparison. The presence of impurities such as amorphous carbon and alloy hydride (MmNi₃-H) catalyst and tubular morphology of the nanotubes can be seen in the FESEM image of as grown MWNT (Fig. S4 (a)). FESEM image of graphite (Fig. S4 (b)) shows its 25 crystalline and highly ordered nature. The FESEM image of purified MWNT displayed in Fig. 2 (a) confirms the absence of impurities by air oxidation and acid treatment. In the FESEM image of L-ARGO (Fig. 2(c)), highly wrinkled morphology and less number of layers can be seen. Uniform distribution as well as 30 small particle size of Pt nanoparticles on f-MWNT and L-ARGO shown in Fig. 2 (b & d), which suggests the suitability of polyol reduction method for the decoration of Pt nanoparticles.

TEM images of MWNT (Panel (a) of Fig. 3) which shows its tubular morphology with hollow cores whereas that of L-ARGO ³⁵ (panel (c) of Fig. 3) shows wrinkled structure which strongly supports the observations made from FESEM images. TEM images displayed in Fig. 3 (b & d) and HRTEM images displayed

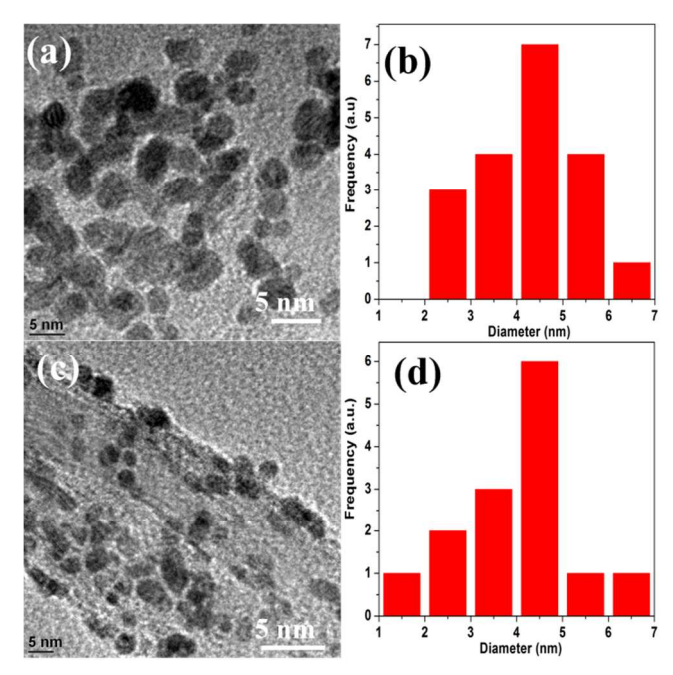


Fig.4 HRTEM images and particle size histograms of (a & b) Pt/L-ARGO, (c & d) Pt/f-MWNT.

in Fig. 4 (a & c) show assembly of non agglomerated ultrafine Pt nanoparticles on the tubular surface of f-MWNT and on thin, flat sheets with occasional wrinkles and folding (L-ARGO). The histograms displayed in Fig. 4 (b & d) show diameter of maximum number of Pt nanopatricles is in the range of 4-6 nm for Pt/f-MWNT and Pt/ L-ARGO.

3.2 Electrochemical analysis

Cyclic voltammetry (CV) is a commonly used tool for assessing the electrocatalytic activity of the electrocatalysts. Fig. 5 shows the cyclic voltammogram of Pt/L-ARGO. CV has been recorded in the potential range from -0.2 t o 1.2 V vs. Ag/AgCl at a scan rate of 50 mV s⁻¹ in aqueous solution of 1 M H₂SO₄. Hydrogen adsorption/desorption peaks are used to evaluate the ECSA

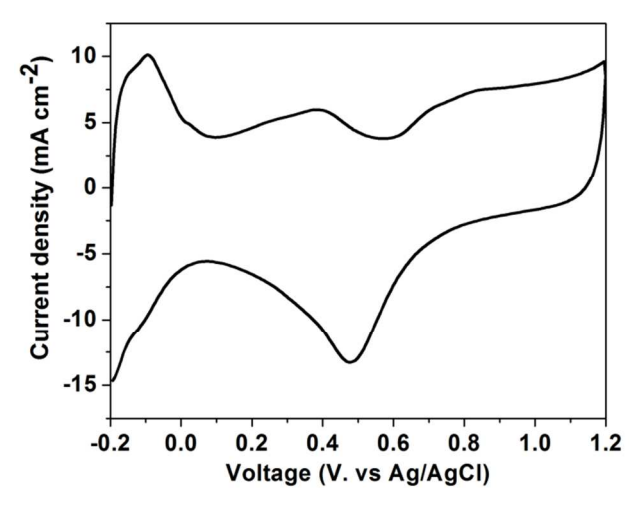


Fig.5 Cyclic volttammogram of Pt/L-ARGO in1 molar H₂SO₄

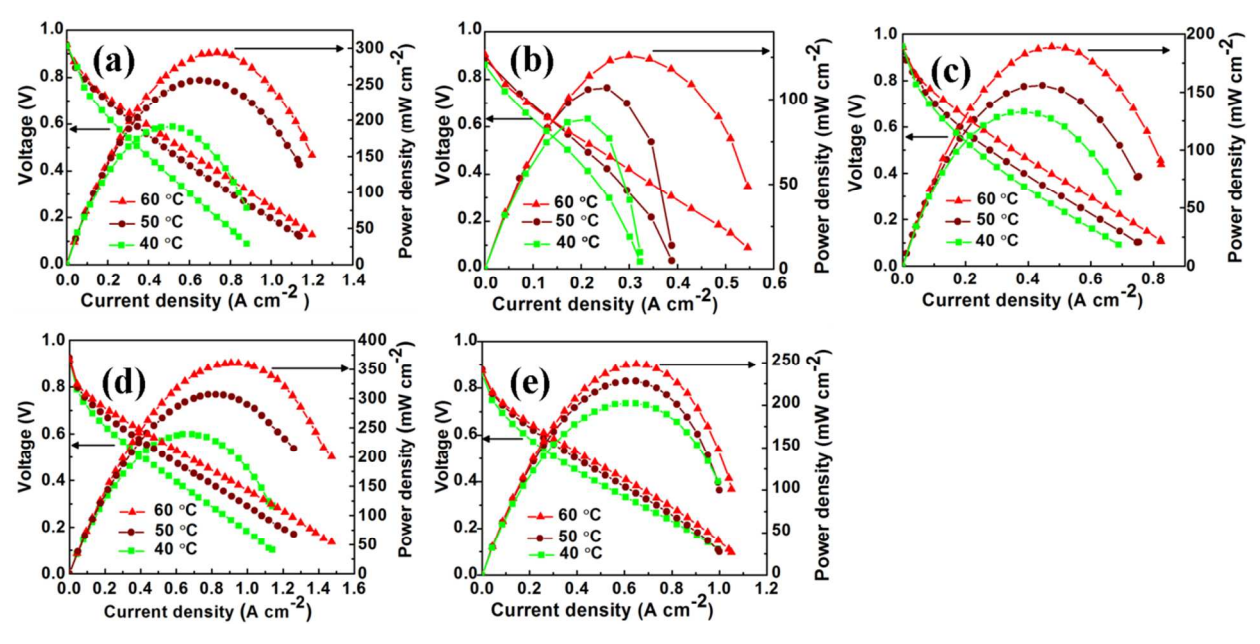


Fig.6Polarization curves recorded at 40 °C, 50 °C and 60 °C without back backpressure for (a) MEA 1, (b) MEA 2, (c) MEA 3, (d) MEA 4 and (e) MEA 5

by employing the equation $(1)^{32}$

10

$$ECSA = Q_H/(0.21 \times [Pt])$$
 -----(1)

where [Pt] represents the loading of Pt and 0.21 mC cm⁻² is the charge required to oxidize a monolayer of H₂ on the Pt site, Q_H is the mean value of the charge exchanged during electro adsorption and desorption of H₂ on the Pt sites. ECSA calculated for Pt/L-ARGO is 40.6m²/g indicates platinum sites are accessible for hydrogen adsorption and desorption reactions. The peak at approximately 0.3V-0.4V is due to the phenolic and ester groups (surface oxides present in graphene).²⁷

20 3.3 Polarization Studies

Table 2. Power density obtained at different temperatures and without backpressure, one atmospheric pressure.

MEA	Power density without backpressure ^a (mW cm ⁻²)		Power density with 1 atm. backpressure ^b (mW cm ⁻²)			
	40 °C	50 °C	60 °C	40 °C	50 °C	60 °C
1	191	256	294	297	356	407
2	88	107	126	125	136	184
3	133	156	189	210	265	306
4	239	307	361	351	429	532
5	202	228	248	299	312	341

 $^{^{\}rm a}$ Power density is taken from polarization curves recorded, which is displayed in Fig. 5

^b Power density is taken from polarization curves recorded, which is displayed in †ESI (Fig. S5).

A systematic and detailed study has been conducted for 30 investigating the electrocatalytic activity of Pt/L-ARGO. MEAs have been fabricated and single cell measurements have been carried out as explained in the experimental section. Fig. 6 (a-e) represents the polarization curves recorded at temperatures 40 °C, 50 °C and 60 °C, without back pressure for all MEAs (MEAs 1-35 5). Polarization curves recorded under similar experimental conditions with one atmospheric backpressure for MEAs 1-5 have been provided in †ESI (Fig. S6 (a-e)). The maximum power densities obtained under various conditions have been tabulated in Table2. Pt nanoparticles decorated graphene as ORR 40 electrocatalyst have been reported already in literature. Maximum power density reported for Pt nanoparticles decorated graphene prepared by chemical reduction method is (161mW cm⁻²)²⁶ low in comparison to power densities obtained (407, 184, 306 mW cm⁻²) for MEAs (1-3) at 60 °C, one atmospheric pressure. Also, 45 maximum power density reported for Pt nanoparticles decorated functionalized hydrogen exfoliated graphene at 60 °C, without back pressure (112 mW cm⁻²)³³ is low in comparison to power densities obtained (294 mW cm⁻², 126 mW cm⁻², 189 mW cm⁻²) for MEAs (1-3) at 60 °C, without back pressure. The above 50 results clearly emphasize the higher ORR activity of Pt/L-ARGO with respect to existing chemically reduced Pt decorated graphene composites. The increase in performance can be attributed to the method adopted for the synthesis of graphene which avoids restacking by removing π-π interaction and uniform 55 decoration of Pt nanoparticles over L-ARGO.

Furthermore, comparison of power densities of MEA 1 and MEA 3 shows an enhancement when Pt/f-MWNT as anode electrocatalyst than Pt/L-ARGO as anode electrocatalyst. This can be due to the lower electrical conductivity of graphite oxide

35

(insulator) reduced graphene in comparison to MWNT, which in turn reduce the electrocatalytic activity. Performance of MEA 2 reduces 55% (at 60 °C, one atmospheric pressure) and 57% (at 60 °C, without backpressure) in comparison to MEA 1 by 50% 5 reductions in Pt loading (at 60 °C, one atmospheric pressure).

In addition to that, till now no single cell measurement has been reported with Pt decorated graphene as anode electrocatalyst. The present work carried polarization studies with Pt/L-ARGO as anode electrocatalyst and Pt/f-MWNT (MEA 10 4 and MEA 5). MEA 4 shows a 31% enhancement in performance (at 60 °C, one atmospheric pressure) with respect to MEA 1, where Pt/L-ARGO has been used as cathode electrocatalyst and Pt/f-MWNT as anode electrocatalyst. Comparison of power densities of MEA 4 and MEA 5 shows that 15 performance of MEA 5 lowers 36 % (at 60 °C, one atmospheric pressure) and 31 % (at 60 °C, without backpressure) with respect to MEA 4 by 50 % reduction in Pt loading. Comparison of power densities of MEA 3 and MEA 5 obtained through polarization studies clearly shows the superior ORR activity of Pt/f-MWNT in 20 comparison to Pt/L-ARGO. Hence the study concludes that MWNT, which is synthesized over MmNi₃ alloy hydride catalyst is a better electrocatalyst support in comparison to graphene obtained by chemical reduction of graphite oxide in the experimental conditions described in section 2.4.

Despite the low electrocatalytic activity of Pt/L-ARGO, easy, environmentally benign as well as cost effective synthesis of L-ARGO makes it a promising electrocatalyst support in comparison to f-MWNT.

The kinetic parameters of the single cell measurement were 30 evaluated by

$$E = E_0 - blog(i) - Ri \qquad ----(2)$$

where E is the cell potential, E_0 is a constant, which is dependent on the cell operating conditions and the cathode electrocatalyst, b is the Tafel slope, R is the ohmic resistance in the electrode and

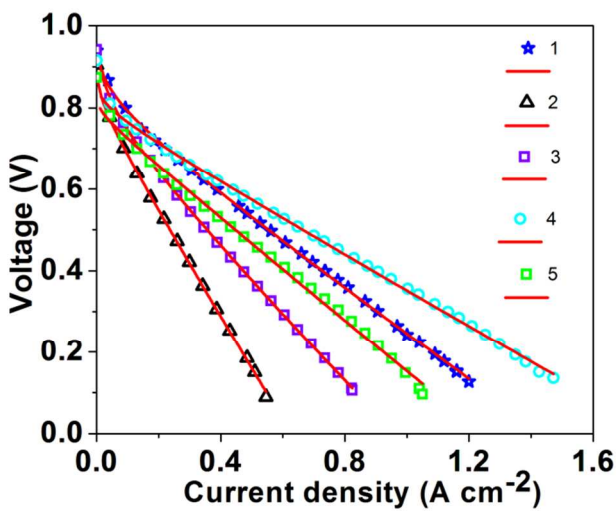


Fig. 7Non-lenear curve fit of experimental data recorded at 60° C, without back pressure using semi empirical relation $E = E_0 - blog(i) - Ri$

electrolyte, i is the current density. The polarization data at 60 $^\circ$ C, without back pressure were fitted to the semi empirical

equation by a non-linear least-squares method in order to evaluate the kinetic parameters, which are displayed in Fig. 7. The results are displayed in Table 3. Single cell measurement with MEA 4 shows lowest dc resistance in comparison to single cells with rest of the MEAs.

Table 3. Kinetic parameters for fuel cells calculated by method of least-50 squares fit of experimental data recorded at 60°C with semi empirical relation $E = E_0 - blog(i) - Ri$, without back pressure.

MEA	R (ohm cm ²)	b (V dec-1)	
1	0.53	0.071	
2	1.23	0.048	
3	0.76	0.096	
4	0.43	0.031	
5	0.62	0.018	

3.4 Stability analysis

Stability of the prepared MEAs have been investigated by running the MEA for a period of 20 hours at a constant voltage of 0.5 V, 60 °C without back pressure. The current density versus time has been recorded to investigate the stability of the MEAs. Fig. 8 shows the stability analysis of MEAs (1-5). The results suggest that all the MEAs show considerable stability for good period of time.

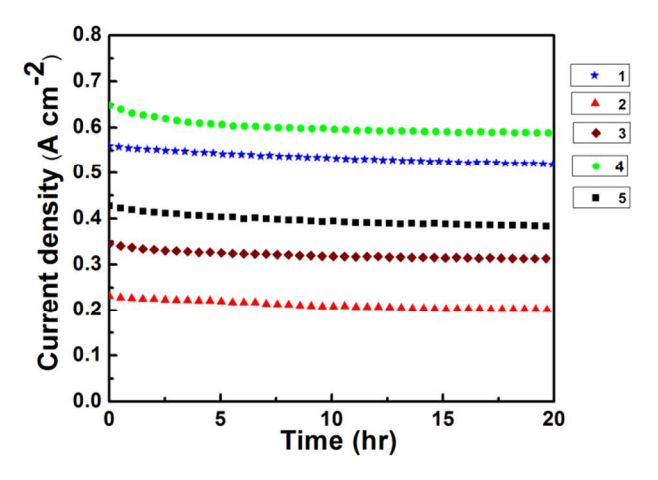


Fig.8Stability studies of MEAs (1-5) at 60 °C, 0.5 V and without back pressure

4. Conclusion

In summary, L-ARGO has been synthesized from graphite oxide by applying an environmentally benign approach. The fuel cell power densities, examined from polarization curves recorded from a series of fabricated MEAs, wherein L-ARGO is the support for Pt, provide an insight into the superior ORR activity of Pt nanoparticles decorated L-ARGO as compared to the chemically reduced Pt-graphene composites. Even though Pt nanoparticles decorated L-ARGO shows a lower ORR and HOR activities in comparison to that of Pt/f-MWNT, considering the

ease and the green approach for the synthesis process, L-ARGO can be considered as a promising low cost electrocatalyst support in PEMFC.

Acknowledgement

5 The authors wish to thank IIT Madras, India for supporting this work. One of the authors is thankful to CSIR, India for SRF assistance. The authors also wish to thank SAIF IIT Madras for FTIR characterization.

10 Notes and references

Alternative Energy and Nanotechnology Laboratory (AENL), Nano Functional Materials Technology centre (NFMTC), Department of Physics, Indian Institute of Technology Madras, India. Fax: XX XXXX XXXX; Tel: +91-44-22574862; E-mail: ramp@iitm.ac.in

15 † Electronic Supplementary Information (ESI) available: [XRD of (as grown MWNT, air oxidized MWNT, MWNT, f-MWNT, graphite, GO. L-ARGO), Raman and FTIR spectra of (MWNT, f-MWNT, graphite, GO and L-ARGO), table containing I_D/I_G calculated from Raman spectra. SEM images of as grown MWNT, graphite, polarization curves recorded 20 at 40 °C, 50 °C, 60 °C, with one atmospheric back pressure]. See

DOI: 10.1039/b000000x/

~

References

- 1. N. M. P. N. R. Markovic and P. N. Ross, *CATTECH*, 2000, **4**, 110-15 126.
- H. A. Gasteiger, S. S. Kocha, B. Sompalli and F. T. Wagner, *Applied Catalysis B: Environmental*, 2005, 56, 9-35.
- 3. R. F. Service, Science, 2007, 315, 172-172.
- C. J. Zhong, J. Luo, B. Fang, B. N. Wanjala, P. N. Njoki, R.
 Loukrakpam and J. Yin, *Nanotechnology*, 2010, 21, 062001-062010.
- D. Puthusseri, T. T. Baby, V. Bhagavathi Parambhath, R. Natarajan and R. Sundara, *International Journal of Hydrogen Energy*, 2013, 38, 6460-6468
- 6. A. L. Dicks, Journal of Power Sources, 2006, 156, 128-141.
- 35 7. S. Iijima, Nature, 1991, 354, 56-58.
 - J. G. Nam, Y. J. Park, B. S. Kim and J. S. Lee, *Scripta Materialia*, 2010, 62, 148-150.
 - 9. C. Du and N. Pan, Journal of Power Sources, 2006, 160, 1487-1494.
- 10. J. Chen, Y. Liu, A. I. Minett, C. Lynam, J. Wang and G. G. Wallace, *Chemistry of Materials*, 2007, **19**, 3595-3597.
- 11. G. Girishkumar, K. Vinodgopal and P. V. Kamat, *The Journal of Physical Chemistry B*, 2004, **108**, 19960-19966.
- 12. C. Wang, M. Waje, X. Wang, J. M. Tang, R. C. Haddon and Yan, *Nano Letters*, 2003, **4**, 345-348.
- 45 13. G. Girishkumar, M. Rettker, R. Underhile, D. Binz, K. Vinodgopal, P. McGinn and P. Kamat, *Langmuir*, 2005, 21, 8487-8494.
 - 14. Y. Chen, J. Wang, H. Liu, M. N. Banis, R. Li, X. Sun, T.-K. Sham, S. Ye and S. Knights, *The Journal of Physical Chemistry C*, 2011, **115**, 3769-3776.
- 50 15. K. A. Worsley, I. Kalinina, E. Bekyarova and R. C. Haddon, *Journal of the American Chemical Society*, 2009, 131, 18153-18158.
 - 16. K. Lee, J. Zhang, H. Wang and D. P. Wilkinson, *Journal of Applied Electrochemistry*, 2006, **36**, 507-522.
 - 17. A. K. Geim and K. S. Novoselov, Nat. Mater., 2007, 6, 183-191.

- A. Kaniyoor, T. T. Baby and S. Ramaprabhu, *Journal of Materials Chemistry*, 2010, 20, 8467-8469.
 - V. Eswaraiah, S. S. Jyothirmayee Aravind and S. Ramaprabhu, Journal of Materials Chemistry, 2011, 21, 6800-6803.
- A. Kaniyoor, T. T. Baby, T. Arockiadoss, N. Rajalakshmi and S.
 Ramaprabhu, *The Journal of Physical Chemistry C*, 2011, 115, 17660-17669.
- S. Stankovich, D. A. Dikin, R. D. Piner, K. A. Kohlhaas, A. Kleinhammes, Y. Jia, Y. Wu, S. T. Nguyen and R. S. Ruoff, *Carbon*, 2007, 45, 1558-1565.
- 65 22. H.-J. Shin, K. K. Kim, A. Benayad, S.-M. Yoon, H. K. Park, I.-S. Jung, M. H. Jin, H.-K. Jeong, J. M. Kim, J.-Y. Choi and Y. H. Lee, *Advanced Functional Materials*, 2009, 19, 1987-1992.
- S. S. Jyothirmayee Aravind, R. Imran Jafri, N. Rajalakshmi and S. Ramaprabhu, *Journal of Materials Chemistry*, 2011, 21, 18199-18204.
- R. Kou, Y. Shao, D. Wang, M. H. Engelhard, J. H. Kwak, J. Wang,
 V. V. Viswanathan, C. Wang, Y. Lin, Y. Wang, I. A. Aksay and J.
 Liu, Electrochemistry Communications, 2009, 11, 954-957.
- 25. R. I. Jafri, T. Arockiados, N. Rajalakshmi and S. Ramaprabhu, Journal of The Electrochemical Society, 2010, 157, B874-B879.
- B. Seger and P. V. Kamat, The Journal of Physical Chemistry C, 2009, 113, 7990-7995.
- Y. Si and E. T. Samulski, Chemistry of Materials, 2008, 20, 6792-6797.
- 80 28. C. V. Rao, A. L. M. Reddy, Y. Ishikawa and P. M. Ajayan, *Carbon*, 2011, 49, 931-936.
- W. S. Hummers and R. E. Offeman, Journal of the American Chemical Society, 1958, 80, 1339-1339.
- 30. J. Zhang, H. Yang, G. Shen, P. Cheng, J. Zhang and S. Guo, Chemical Communications, 2010, 46, 1112-1114.
- A. L. M. Reddy, M. Shaijumon and S. Ramaprabhu, *Nanotechnology*, 2006, 17, 5299.
- 32. A. Pozio, M. De Francesco, A. Cemmi, F. Cardellini and L. Giorgi, *Journal of Power Sources*, 2002, **105**, 13-19.
- 90 33. S. S. J. Aravind and S. Ramaprabhu, ACS Applied Materials & Interfaces, 2012, 4, 3805-3810.